


Molecular characteristics and pathogenic assessment of porcine epidemic diarrhoea virus isolates from the 2018 endemic outbreaks on Jeju Island, South Korea

Sunhee Lee¹ | Dong-Uk Lee² | Yun-Hee Noh² | Seung-Chul Lee² | Hwan-Won Choi² |
 Hyoung-Seok Yang³ | Jun-Ho Seol⁴ | Seong Hwan Mun⁴ | Won-Myoung Kang⁴ |
 Hyekyung Yoo⁵ | Changhee Lee¹ 

¹Animal Virology Laboratory, School of Life Sciences, BK21 plus KNU Creative BioResearch Group, Kyungpook National University, Daegu, Republic of Korea

²ChoongAng Vaccine Laboratories, Daejeon, Republic of Korea

³Veterinary Research Institute, Jeju Special Self-Governing Province, Jeju, Republic of Korea

⁴Animal Health Division, Jeju Special Self-Governing Province, Jeju, Republic of Korea

⁵Farm & Pharm Veterinary Hospital, Jeju, Republic of Korea

Correspondence

Changhee Lee, Animal Virology Laboratory, School of Life Sciences, College of Natural Sciences, Kyungpook National University, Daegu 41566, Republic of Korea.
 Email: changhee@knu.ac.kr

Funding information

National Research Foundation of Korea, Grant/Award Number: NRF-2018R1D1A1B07040334

Abstract

Since the 2013–2014 incursion of the virulent G2b porcine epidemic diarrhoea virus (PEDV) pandemic strains in South Korea, frequent moderate-scale regional outbreaks have recurred. In particular, areas of Jeju Island with extensive swine production have faced repeated epidemics since the re-emergence in 2014. The current study reports the complete genome sequences and molecular characterization of the representative PEDV strains responsible for the 2018 endemic outbreaks on Jeju Island. All isolates were determined to belong genetically to the highly pathogenic pandemic G2b group. Full-length genome sizes of four isolates differed from that of the G2b epidemic field strain due to insertion or deletion (DEL) mutations in the non-structural protein (nsp)- or spike (S) protein-coding regions. The 2018 Jeju isolates shared 96.7%–98.7% and 98.5%–99.4% identity at the S gene and whole-genome levels, respectively, compared to global G2b PEDV strains. Genetic and phylogenetic analyses indicated that the 2018 isolates were closest to the 2014 G2b re-emergent Jeju strains, but appeared to have undergone substantial rapid independent evolution. Among the isolates, a notable nsp3 DEL variant strain, KOR/KNU-1807/2018, was isolated and propagated by continuous passages in Vero cells, and displayed typical PEDV-induced syncytia formation. Genomic sequencing identified a unique 8-nt DEL in the extreme C-terminal region of the S gene at the 4th passage (KNU-1807-P4) compared to its original sample. This DEL resulted in the premature termination of S by nine amino acid residues (EVFEKVHVQ), which contained a KxHxx motif that is a potential endoplasmic reticulum retrieval signal. In vivo animal studies showed that variant strain KNU-1807 had decreased virulence in suckling piglets. These results advance our knowledge regarding the genetic variation and pathogenicity of the G2b PEDV endemic strains prevalent in Jeju swine herds in South Korea.

KEYWORDS

endemic outbreaks, genome analysis, pathogenicity, PEDV, virus isolation

1 | INTRODUCTION

Porcine epidemic diarrhoea virus (PEDV) is a highly-contagious and deadly enteric swine coronavirus and is considered an emerging and re-emerging viral pathogen that is a financial threat to the global pork industry (Lee, 2015, 2019; Stevenson et al., 2013; Weng, Weersink, Poljak, de Lange, & von Massow, 2016). PEDV belongs to the genus *Alphacoronavirus* in the family Coronaviridae of the order Nidovirales (Gorbalenya, Enjuanes, Ziebuhr, & Snijder, 2006; Saif, Pensaert, Sestack, Yeo, & Jung, 2012). The PEDV genome is approximately 28-kb long with a 5' cap and 3' polyadenylated tail and is composed of a 5'-untranslated region (UTR), at least seven open reading frames (ORFs) designated ORF1a, ORF1b, and ORFs 2 through 6 and a 3'-UTR. The first two large ORFs, ORF1a and 1b, encode replicase polyproteins that undergo autoproteolysis by viral proteases to eventually produce 16 processing non-structural proteins (nsp1–16). The remaining ORFs encode four canonical coronavirus structural proteins, spike (S), membrane (M), envelope (E) and nucleocapsid (N), as well as a single accessory gene, ORF3 (Lee, 2015, 2019).

Since its emergence in South Korea in 1992, small- to large-scale PEDV epizootics have occurred annually throughout the nation, leading to substantial economic losses in domestic pig production (Lee, 2015, 2019). The 2013 PED pandemic that ravaged the United States (Stevenson et al., 2013) also struck the Korean Peninsula and decimated more than 40% of the pig farms across the country during 2013–2014 (Lee, 2015, 2019; Lee et al., 2014; Lee & Lee, 2014). Subsequently, in late March 2014, the virus invaded Jeju Island located 80 km from the South Korea mainland at the closest point, which had maintained PEDV-naïve status for a decade, causing massive neonatal mortality in provincial herds. Genetic and phylogenetic analyses revealed that the re-emergent Jeju Island PEDV isolates were most closely related to the pandemic genogroup 2b (G2b) strains that were responsible for the 2013–2014 global outbreaks, suggesting a direct introduction of the virus from the mainland of South Korea via unknown contaminating sources (Lee et al., 2014). Even with province-wide vaccination or intentional virus-exposure practices being implemented in order to provide herd immunity around the areas that contain dense swine populations, PEDV has continued to plague the provincial pork industry. Since several pig farms have experienced recurrent PEDV outbreaks within a single year, PED has become endemic on Jeju Island (Lee et al., 2014; Lee & Lee, 2017). In this study, we determined the complete genome sequences of field isolates on Jeju Island to investigate the diversity of the PEDVs responsible for the ongoing endemic outbreaks. Additionally, we isolated and serially cultured a novel PEDV strain, KOR/KNU-1807/2018, in cell culture and investigated its genotypic and phenotypic characteristics in vitro and in vivo.

2 | MATERIAL AND METHODS

2.1 | Clinical sample collection

In early 2018, mild sporadic suspect-PEDV outbreaks with low mortality rates in newborn piglets occurred on several farms in

the Hallim and Daejeong areas of Jeju Province. Small intestine (SI) specimens were collected at 18 different pig farms located in those districts from January through June 2018 from dead piglets that had acute diarrhoea. Intestinal homogenates were prepared as 10% (wt/vol) suspensions in phosphate-buffered saline (PBS) using a MagNA Lyser Instrument (Roche Diagnostics, Mannheim, Germany) with three rounds of 15 s at a force of 8,000 g. The suspensions were then vortexed and centrifuged for 10 min at 4,500 g (Hanil Centrifuge FLETA5, Incheon, South Korea). The clarified supernatants were initially subjected to RT-PCR analysis using an *i*-TGE/PED Detection Kit (iNtRON Biotechnology) according to the manufacturer's instructions. PEDV-positive samples were filtered through a 0.22- μ m-pore syringe filter (Millipore) and stored at -80°C until subsequent sequencing analysis and virus isolation were performed.

2.2 | Nucleotide sequence analyses

The S glycoprotein gene sequences of the virus isolates were determined by traditional Sanger methods. Two overlapping cDNA fragments spanning the entire S gene of each isolate were amplified by RT-PCR as previously described (Lee, Park, Kim, & Lee, 2010). The individual cDNA amplicons were gel-purified, cloned using the pGEM-T Easy Vector System (Promega) and sequenced in both directions using two commercial vector-specific T7 and SP6 primers and gene-specific primers. In addition, the complete genomes of representative PEDV field strains were also sequenced. Ten overlapping cDNA fragments spanning the entire genome of each virus strain were RT-PCR-amplified as described previously (Lee, Kim, & Lee, 2015; Lee & Lee, 2014; Lee et al., 2017) and each PCR product was sequenced as described above. The 5' and 3' ends of the genomes of the individual isolates were determined by rapid amplification of cDNA ends (RACE) as described previously (Lee & Lee, 2013). The full-length S gene or whole-genome sequences of the 2018 viruses have been deposited in the GenBank database under the accession numbers shown in Figure 2a.

2.3 | Multiple alignments and phylogenetic analyses

The sequences of 66 fully sequenced S genes and 39 complete genomes of global PEDV isolates were independently used in sequence alignments and phylogenetic analyses. Multiple sequence alignments were generated using the ClustalX 2.0 program (Thompson, Gibson, Plewniak, Jeanmougin, & Higgins, 1997) and the percentages of nucleotide sequence divergences were assessed using the same software. Phylogenetic trees were constructed from the aligned nucleotide or amino acid sequences using the neighbour-joining method and subsequently subjected to bootstrap analysis with 1,000 replicates to determine the percentage reliability values of each internal node of the tree (Saitou & Nei, 1987). All phylogenetic trees were generated using Mega 4.0 software (Tamura, Dudley, Nei, & Kumar, 2007).

2.4 | Virus isolation

Porcine epidemic diarrhoea virus isolation was performed using Vero cells in the presence of trypsin (USB) as described previously (Lee et al., 2015). Briefly, inocula were prepared by adding trypsin (USB) to intestinal suspensions to a final concentration of 10 µg/ml. Confluent Vero cells grown in 6-well plates were washed with PBS and inoculated with 400 µl of each trypsin-containing inoculum. After incubating at 37°C for 1 hr to allow for viral adsorption, 2 ml of virus growth medium consisting of alpha minimum essential medium (α-MEM; Invitrogen) supplemented with antibiotic-antimycotic solutions (100×; Invitrogen), 0.3% tryptose phosphate broth (TPB; Sigma), 0.02% yeast extract (Difco), 10 mM HEPES (Invitrogen) and 5 µg/ml of trypsin was added to each well. The inoculated cells were maintained at 37°C under 5% CO₂ and monitored daily for cytopathic effects (CPE). When ~70% of cells showed CPE, the infected cells were subjected to three rounds of freezing and thawing. The culture supernatants were then collected and centrifuged for 10 min at 400 g and filtered through a 0.22-µm pore filter. The clarified supernatants were aliquoted and stored at -80°C as passage 1 (P1) viral stocks for use in plaque purification and subsequent serial passaging. If CPE and RT-PCR results were negative after five blind passages, virus isolation was considered negative for those samples.

2.5 | Immunofluorescence assay (IFA)

Vero cells grown on microscope coverslips placed in 6-well tissue culture plates were mock infected or infected with PEDV at a multiplicity of infection (MOI) of 0.1. The virus-infected cells were cultured until 24 hr, fixed with 4% paraformaldehyde for 10 min at room temperature (RT) and permeabilized with 0.2% Triton X-100 in PBS at RT for 10 min. The cells were blocked with 1% bovine serum albumin (BSA) in PBS for 30 min at RT and then incubated for 2 hr with a monoclonal antibody (MAb) specific for PEDV N protein (ChoongAng Vaccine Laboratories). After being washed five times with PBS, the cells were incubated for 1 hr at RT with a goat anti-mouse secondary antibody conjugated to Alexa Fluor 488 (Invitrogen) followed by counterstaining with 4',6-diamidino-2-phenylindole (DAPI; Sigma). The coverslips were mounted onto glass microscope slides using mounting buffer and the stained cells were visualized using a fluorescence Leica DM IL LED microscope (Leica).

2.6 | Virus titration

Vero cells were infected with each passage of KNU-1807 virus stock in the presence of trypsin as described above. The culture supernatants were collected at 24 or 48 hr post-infection (hpi) when 70% CPE had commonly developed. For growth kinetics experiments, supernatants were harvested from cells infected with each selected passage virus at various time points (6, 12, 24, 36 and 48 hpi) and

stored at -80°C. Virus titres were measured by end-point titration in 96-well plates using 10-fold serial dilutions of the samples in triplicate for each dilution to determine the amount of virus required to produce CPE in 50% of the inoculated Vero cells. The 50% tissue culture infectious dose (TCID₅₀) per ml of virus stock was calculated using the Reed-Muench method (Reed & Muench, 1938).

2.7 | Quantitative real-time RT-PCR

Viral RNA was extracted from virus supernatants from infected Vero cells and faecal specimens using an i-TGE/PED Detection Kit according to the manufacturer's protocol. Quantitative real-time RT-PCR was performed using a One Step PrimeScript RT-PCR Kit (TaKaRa) and primers (forward primer 5'-ACGTCCCTTACTTTCAATTCACA-3', reverse primer 5'-TATACTTGGTACACACATCCAGAGTCA-3') and a probe (5'-FAM-TGAGTTGATTACTGGCAGCCTAAACCAC-BHQ1-3') described elsewhere (Kim et al., 2007; Lee et al., 2017; Sagong & Lee, 2011). Amplification of the reaction mixtures was performed using a Thermal Cycler Dice Real Time System (TaKaRa) and the results were analysed using software as described previously (Lee et al., 2017; Sagong & Lee, 2011).

2.8 | Pig infection experiments

The in vivo swine studies were performed at the ChoongAng Vaccine Laboratory Animal Facility under the guidelines established by its Institutional Animal Care and Use Committee. A total of nine 3-day-old suckling piglets were obtained from commercial cross-bred sows (Great Yorkshire × Dutch Landrace) at a conventional breeding farm with a good health record and either vaccinated against PEDV or no known prior PED outbreak. All animals were confirmed negative for PEDV, transmissible gastroenteritis virus (TGEV), porcine deltacoronavirus and porcine rotaviruses by virus-specific RT-PCR analysis of rectal swabs and determined to be free of antibodies to PEDV, TGEV and porcine reproductive and respiratory syndrome virus (PRRSV) by serum neutralization tests as described previously (Lee et al., 2017) and a commercial PRRSV antibody ELISA kit (HerdChek PRRS X3; IDEXX Laboratories). Pigs were randomly assigned to three experimental groups: the highly virulent KNU-141112-P5-inoculated group ($n = 3$) (Lee et al., 2015), the KNU-1807-P10-inoculated group ($n = 4$) and the sham-inoculated control group ($n = 2$). Animals were fed commercial milk replacer (3–4 times daily) and had ad libitum access to water for the 5-day duration of the study. Following a 2-day acclimation period, piglets (5-day old) in the virus-inoculated groups received an oral 1-ml dose of 10^{3.0} TCID₅₀/ml of the appropriate virus, which was equivalent to 100 median pig diarrhoea dose PDD₅₀ of KNU-141112 (Baek et al., 2016; Lee et al., 2015, 2017). The sham-inoculated pigs were administered with cell culture media as a placebo. Animals were monitored three times daily throughout the experiment for clinical signs of vomiting and diarrhoea and for mortality. Stool samples from the pigs in all groups were collected prior to inoculation and thereon daily using 16-inch cotton-tipped swabs. The PEDV faecal shedding titres were determined by real-time RT-qPCR

as described above. A PEDV isolate with a known infectivity titre was 10-fold serially diluted to generate a standard curve in each PCR plate. The virus concentrations (TCID₅₀/ml) in the samples were calculated based on the standard curve. The mean cycle threshold (Ct) values were calculated for the PCR-positive samples and the mean virus titres were calculated for all pigs within the group. A clinical significance score (CSS) was determined using the following scoring criteria for diarrhoeal severity based on visual examination for 5 days post-inoculation (dpi): 0, normal with no diarrhoea (mean Ct values > 45); 1, mild with fluidic faeces; 2, moderate mucus to watery diarrhoea; 3, severe watery and projectile diarrhoea (mean Ct values < 20); 4, death. The piglets were necropsied upon death after challenge throughout the study, whereas all surviving pigs from the challenge and control groups were killed at five days post-challenge for post-mortem examinations.

2.9 | Histopathology and immunohistochemistry of the small intestines

At necropsy, small intestine tissue specimens (<3 mm thick) were collected from each piglet, fixed in 10% formalin for 24 hr at RT, and embedded in paraffin according to standard laboratory procedures. The formalin-fixed paraffin-embedded tissues were cut at 5–8- μ m thick sections using a microtome (Leica), floated in a 40°C water bath containing distilled water, and transferred to glass slides. The tissues were then deparaffinized in xylene for 5 min and rehydrated in decreasing concentrations of ethanol (100%, 95%, 90%, 80% and 70%, respectively) for 3 min each. The deparaffinized intestinal tissue sections were stained with haematoxylin and eosin (Sigma) for histopathology or subjected to immunohistochemistry (IHC) using PEDV N-specific MAb as described previously (Lee et al., 2015, 2017). Villous height and crypt depth were also measured throughout the H&E-stained jejunal sections and the mean ratio of jejunal villous height to crypt depth (VH:CD) was calculated as described previously (Jung, Kim, Ha, Choi, & Chae, 2006).

2.10 | Statistical analysis

All values are expressed as the means \pm standard deviation of the means (SDM). All statistical significances were evaluated by a Student's *t* test by using GraphPad Prism software version 5.0 (GraphPad Prism Inc.). *p*-values of <0.05 were considered statistically significant.

3 | RESULTS

3.1 | Genetic and phylogenetic characterization of 2018 Jeju PEDV strains

TGE/PED detection kit-based RT-PCR assays revealed that all the samples were positive for PEDV. Subsequently, we were able to determine the complete S gene sequences of the 2018 Jeju isolates

from the 11 PED-endemic farms using traditional Sanger sequencing methods. The 2018 Jeju strains designated as KNU-1804 to KNU-1807 and KNU-1815 to KNU-1821 had 4,161 nucleotides (nt) long S genes predicted to encode a 1,386-amino acid (aa) protein, except for KNU-1816. Interestingly, the KNU-1816 virus possessed a unique 4-aa (KSGL) insertion at position 232 in the S1 domain, which was completely absent in the genome sequences of the other G1 and G2 strains available in the GenBank database. Compared to the prototype CV777 strain (Lee, 2015; Lee et al., 2010), all the Jeju isolates contained the genetic signature of the G2 field strains with S insertions-deletions (S INDELS) (Figure S1). Further sequencing analysis suggested small-scale genetic variations among the eleven 2018 strains with 96.8%–100% homology at the amino acid level among them. Moreover, the Jeju Island strains from 2018 also demonstrated 96.7%–98.7% aa identity with the global G2b PEDVs reported previously in Jeju Island, mainland South Korea, and the US, but only 91.3%–92.5% and 94.0%–94.7% aa homology with the classical G1a or variant G1b strains respectively (Table 1). Compared to the 2014 re-emergent Jeju strain KNU-1409, the 2018 Jeju viruses contained a total of 19–26 aa mutations in the S gene (Figure 1a). Remarkably, more than half of these variations were identified only in the 2018 Jeju Island strains (black lines). In particular, KNU-1806, -1807, -1815, -1816 and -1818 each possessed their own unique mutations that did not exist in other domestic strains (black arrow lines) compared. In total, the genetic data indicated that the 2018 Jeju isolates were still most closely related to the G2b pandemic strains but that they continued to independently evolve through the process of genetic drift.

We then sequenced and analysed the complete genomes of seven representative strains to investigate the genetic relatedness between the contemporary Jeju-endemic strains and other global PEDV strains. Among those, whole genomes of only three strains consisted of 28,038 nt (excluding the 3' poly(A) tail), which was the genome size of most G2b field viruses. However, the genome of KNU-1816 was longer with 28,050 nt, while the genome sequences of KNU-1807, -1815, and -1818 were each shorter and 28,017, 28,029 and 28,035 nt respectively. The longer genome of KNU-1816 was ascribed to a 4-aa insertion in the S protein as described above, whereas the shorter genome sizes of KNU-1807 and -1815 resulted from unique 21-nt (7-aa) or 9-nt (3-aa) deletion (DEL) at genomic positions 3,324–3,344 or 3,408–3,416 located in ORF1a encoding nsp3, respectively (Figure 1b), which serves as a papain-like protease (PL^{PRO}). Intriguingly, additional sequence analysis of isolates KNU-1820 and KNU-1821, which were found to be most closely genetically and geographically related to KNU-1815, revealed the acquisition of identical 3-aa DEL mutations in nsp3, suggesting direct transmission of the homologous strain among these farms (Figure 1a and b). The remaining strain KNU-1818 possessed a 3-nt (1-aa) DEL at genomic positions 10,575–10,577 in ORF1a encoding nsp6. Except for the S-insertion in KNU-1816, the nsp3-DEL in KNU-1807, -1815, -1820 and -1821, and the nsp6-DEL in KNU-1818, no additional INDELS were identified throughout the entire genome.

TABLE 1 Pairwise comparisons of nucleotide and amino acid sequences of the S protein genes of the 2018 Jeju isolates and genogroup representative PEDV strains

Strain name (Genogroup)	CV 777	DR-13/att	OH 851	KNU 1406	KNU 0801	KNU 0901	GD-B	Co/13	IN 17846	IA1	KNU 1305	KNU 141112	KNU 1409	
CV777 (G1a)	-	96.8	95.7	95.7	94.0	93.8	93.8	93.7	93.7	93.7	93.7	93.7	93.6	
DR-13/att G1a)	96.0	-	95.9	95.9	94.1	93.9	93.6	93.5	93.6	93.5	93.5	93.5	93.5	
OH851 (G1b)	96.1	96.1	-	99.9	92.9	93.3	95.8	96.4	96.4	96.4	96.3	96.3	96.2	
KNU-1406 (G1b)	96.2	96.1	99.7	-	92.9	93.3	95.7	96.4	96.3	96.4	96.3	96.2	96.2	
KNU-0801 (G2a)	93.1	93.1	92.5	92.6	-	97.9	94.7	94.7	94.7	94.7	94.6	94.6	94.5	
KNU-0901(G2a)	93.2	92.9	93.0	93.1	97.9	-	95.2	95.1	95.1	95.1	95.1	95.1	95.0	
GD-B (G2b)	93.1	92.5	95.4	95.3	94.1	94.7	-	99.2	99.2	99.2	99.2	99.2	99.2	
Co/13 (G2b)	93.2	92.8	95.8	95.8	94.3	94.8	99.4	-	99.9	99.9	99.8	99.8	99.7	
IN17846 (G2b)	93.2	92.8	95.8	95.8	94.3	94.8	99.4	100.0	-	99.8	99.9	99.9	99.8	
IA1 (G2b)	93.2	92.8	95.8	95.8	94.3	94.8	99.4	100.0	100.0	-	99.8	99.8	99.7	
KNU-1305 (G2b)	93.1	92.7	95.7	95.6	94.1	94.8	99.2	99.8	99.8	99.8	-	99.9	99.8	
KNU-141112 (G2b)	93.0	92.6	95.6	95.6	94.0	94.8	99.2	99.7	99.7	99.7	99.7	-	99.8	
KNU-1409 (G2b)	93.2	92.7	95.8	95.7	94.2	94.8	99.3	99.9	99.9	99.9	99.7	99.7	-	
KNU-1601 (G2b)	92.4	91.9	94.5	94.4	93.3	93.9	98.0	98.5	98.5	98.5	98.4	98.3	98.6	
KNU-1703 (G2b)	92.5	92.0	94.5	94.6	93.7	94.3	97.9	98.2	98.2	98.2	98.1	98.1	98.1	
KNU-1705 (G2b)	92.5	92.5	95.2	95.1	93.8	94.4	98.0	98.5	98.5	98.5	98.4	98.4	98.4	
KNU-1708 (G2b)	93.2	92.7	95.8	95.7	94.0	94.6	98.9	99.4	99.4	99.4	99.2	99.2	99.3	
KNU-1804 (G2b)	92.5	91.8	94.7	94.6	93.4	94.0	97.9	98.4	98.4	98.4	98.3	98.2	98.5	
KNU-1805 (G2b)	92.5	91.8	94.7	94.6	93.4	94.0	97.9	98.4	98.4	98.4	98.3	98.2	98.5	
KNU-1806 (G2b)	92.3	91.7	94.5	94.4	93.1	93.7	97.9	98.4	98.4	98.4	98.2	98.1	98.4	
KNU-1807 (G2b)	92.2	91.6	94.5	94.4	93.1	93.7	97.8	98.4	98.4	98.4	98.2	98.1	98.4	
KNU-1815 (G2b)	92.1	91.4	94.3	94.2	93.2	93.7	98.0	98.3	98.3	98.3	98.1	98.1	98.4	
KNU-1816 (G2b)	92.0	91.4	94.3	94.3	92.9	93.5	97.7	98.2	98.2	98.2	98.1	98.0	98.3	
KNU-1817 (G2b)	92.2	91.6	94.5	94.4	93.1	93.7	97.9	98.4	98.4	98.4	98.3	98.2	98.5	
KNU-1818 (G2b)	91.9	91.3	94.0	94.0	92.8	93.4	97.5	98.1	98.1	98.1	97.9	97.9	98.1	
KNU-1819 (G2b)	92.4	91.7	94.6	94.5	93.2	93.8	98.1	98.6	98.6	98.6	98.4	98.4	98.7	
KNU-1820 (G2b)	92.3	91.7	94.3	94.3	93.6	94.0	97.7	98.1	98.1	98.1	98.0	97.9	98.2	
KNU-1821 (G2b)	92.3	91.7	94.3	94.3	93.6	94.0	97.7	98.1	98.1	98.1	98.0	97.9	98.2	
KNU 1601	KNU 1703	KNU 1705	KNU 1708	KNU 1804	KNU 1805	KNU 1806	KNU 1807	KNU 1815	KNU 1816	KNU 1817	KNU 1818	KNU 1819	KNU 1820	KNU 1821
93.2	93.3	93.3	93.5	93.1	93.1	93.1	93.0	92.9	92.7	93.0	92.9	93.0	93.0	93.0
93.0	93.1	93.2	93.3	92.9	92.9	92.9	92.9	92.7	92.5	92.8	92.8	92.8	92.8	92.9
95.6	95.9	96.2	96.4	95.6	95.6	95.6	95.5	95.4	95.2	95.5	95.3	95.5	95.5	95.5
95.5	96.0	96.2	96.4	95.5	95.5	95.5	95.4	95.4	95.2	95.5	95.2	95.5	95.4	95.4
94.1	94.3	94.4	94.5	94.0	94.0	93.9	93.9	93.9	93.5	94.0	93.9	94.0	94.0	94.0
94.5	94.8	94.8	94.9	94.4	94.4	94.4	94.3	94.4	93.9	94.4	94.3	94.4	94.4	94.4
98.5	98.3	98.4	98.8	98.4	98.4	98.4	98.3	98.3	98.0	98.3	98.2	98.4	98.2	98.3
99.0	98.9	99.1	99.5	98.9	98.9	98.9	98.8	98.8	98.6	98.8	98.7	98.9	98.8	98.8
99.1	98.8	99.0	99.4	99.0	99.0	99.0	98.9	98.9	98.7	98.9	98.8	99.0	98.9	98.9
99.0	98.9	99.0	99.5	98.9	98.9	98.8	98.8	98.7	98.6	98.8	98.7	98.8	98.7	98.8
99.1	98.8	99.0	99.4	98.9	98.9	98.9	98.9	98.8	98.6	98.9	98.8	98.9	98.8	98.8
99.0	98.8	98.9	99.4	98.9	98.9	98.9	98.9	98.8	98.6	98.9	98.7	98.9	98.8	98.8
99.2	98.8	98.9	99.3	99.1	99.1	99.0	99.0	98.9	98.7	99.0	98.9	99.0	98.9	99.0

(Continues)

TABLE 1 Continued

KNU 1601	KNU 1703	KNU 1705	KNU 1708	KNU 1804	KNU 1805	KNU 1806	KNU 1807	KNU 1815	KNU 1816	KNU 1817	KNU 1818	KNU 1819	KNU 1820	KNU 1821
-	98.1	98.1	98.7	98.5	98.5	98.5	98.4	98.4	98.2	98.4	98.4	98.5	98.4	98.4
97.1	-	99.3	98.8	98.1	98.1	98.1	98.1	97.9	97.7	98.1	97.9	98.1	97.9	97.9
97.1	98.4	-	98.9	98.1	98.1	98.1	98.1	98.0	97.7	98.0	97.9	98.1	97.9	98.0
97.9	97.9	98.1	-	98.5	98.5	98.5	98.4	98.4	98.2	98.5	98.3	98.5	98.4	98.4
97.6	97.1	97.4	97.9	-	99.9	99.4	98.4	98.3	98.0	99.5	98.2	99.5	98.3	98.4
97.6	97.1	97.4	97.9	99.9	-	99.4	98.4	98.3	98.0	99.5	98.2	99.5	98.3	98.4
97.5	96.9	97.1	97.8	98.7	98.7	-	98.3	98.2	98.0	99.4	98.2	99.5	98.2	98.2
97.4	97.1	97.1	97.8	97.5	97.5	97.3	-	98.2	98.0	98.3	98.3	98.3	98.2	98.2
97.6	97.1	97.0	97.7	97.4	97.4	97.2	97.4	-	97.9	98.2	98.3	98.2	99.3	99.3
97.4	96.7	96.8	97.6	97.1	97.1	96.9	97.2	97.2	-	98.0	97.8	98.0	97.9	97.9
97.5	96.9	97.1	97.9	98.9	98.9	98.7	97.4	97.4	97.1	-	98.2	99.7	98.2	98.2
97.4	96.8	96.8	97.5	97.0	97.0	96.8	97.4	97.7	96.9	97.1	-	98.2	98.2	98.3
97.6	97.1	97.3	98.0	99.2	99.2	98.9	97.6	97.4	97.3	99.5	97.0	-	98.2	98.2
97.4	96.8	96.9	97.6	97.4	97.4	97.0	97.2	98.8	97.1	97.2	97.3	97.2	-	99.9
97.4	96.8	96.9	97.6	97.4	97.4	97.0	97.2	98.8	97.1	97.2	97.3	97.2	100	-

Note: The percent nucleotide identity was shown in the upper right and the percent amino acid identity was presented in the lower left.

The 2018 Jeju isolates shared a high degree of nucleotide homology with each other (98.8%–99.6%) and the other global G2b PEDV strains (98.5%–99.4%) at the genomic level, showing the highest nucleotide identity with the 2013–2014 Korean epidemic strains (Table 2). The number of nt/aa differences and percentages of shared identity between the 2018 Jeju isolates and the Korean prototype G2b strain KNU-1305 are summarized in Table 3. Compared to the complete genome of KNU-1305, the KNU-1804, -1806, -1807, -1815, -1816, -1817 and -1818 genomes exhibited 166-nt (99.4% homology), 169-nt (99.3% homology), 190-nt (99.3% homology), 191-nt (99.3% homology), 185-nt (99.3% homology), 175-nt (99.3% homology) and 168-nt (99.4% homology) differences, respectively, ultimately resulting in 60, 63, 76, 65, 79, 62 and 73 non-synonymous point mutations respectively (32 in ORFs 1a and 1b, 23 in S, 1 in ORF3, 1 in E, 1 in M, and 2 in N for KNU-1804; 34 in ORFs 1a and 1b, 24 in S, 3 in ORF3, 1 in E, and 1 in N for KNU-1806; 40 in ORFs 1a and 1b, 24 in S, 4 in ORF3, 2 in M, and 6 in N for KNU-1807; 33 in ORFs 1a and 1b, 25 in S, 3 in ORF3, and 4 in N for KNU-1815; 41 in ORFs 1a and 1b, 22 in S, 4 in ORF3, 1 in E, 4 in M, and 7 in N for KNU-1816; 29 in ORFs 1a and 1b, 23 in S, 2 in ORF3, 2 in E, 3 in M, and 3 in N for KNU-1817; and 38 in ORFs 1a and 1b, 28 in S, 1 in ORF3, and 6 in N for KNU-1818).

Subsequent phylogenetic analysis based on the complete S protein sequence clearly delineated the PEDV strains into two distinct genogroup clusters, the classical or recombinant and low-pathogenic group G1 and the field epidemic or pandemic and high-pathogenic group G2. These were further divided into subgroups 1a, 1b, 2a and 2b (Figure 2a). All the 2018 Jeju strains belonged to the subgroup G2b, which clustered closely around the recent and previous Jeju isolates, thereby forming an independent clade within the same subgroup, but were distant from the mainland epidemic strains.

Whole-genome phylogeny indicated that the 2018 Jeju strains grouped within the same cluster as the global epizootic strains (Figure 2b).

3.2 | Virus isolation and in vitro phenotypic and genetic characteristics

We attempted to isolate PEDV from RT-PCR-positive clinical samples using Vero cells. One PEDV isolate, KNU-1807, was isolated from specimens collected from a single 280-sow farrow-to-finishing farm located in the Hallim District and successfully cultivated in cell culture. In infected Vero cells from passage 4 (P4), KNU-1807 produced obvious CPE typical of PEDV infection, such as cell fusion, syncytium formation and cell detachment. Increased syncytia size became more distinct at the 5th passage (P5). Virus propagation was confirmed by the detection of PEDV antigens with IFA using a PEDV N-specific MAb. The apparent staining was localized in the cytoplasm of syncytial cells. In contrast, neither CPE nor N-specific staining was evident in mock-inoculated Vero cells. Examples of CPE and corresponding IFA images from selected passages are shown in Figure 3a. The amount of viral genome in each of the selected passages was further evaluated and the mean Ct value was determined to be 15.07 with a range from 13.52 (P10) to 16.63 (P5). The infectious titre of the isolate was $10^{5.5}$ TCID₅₀/ml at P5 and approximately 10^7 TCID₅₀/ml at the later passages. Analysis of growth kinetics further demonstrated that KNU-1807 replicated rapidly and efficiently in Vero cells, reaching a titre $>10^6$ TCID₅₀/ml by 12 hpi (Figure 3b).

In addition, we sequenced the coding region of nsp3 and the entire S gene of strain KNU-1807 at the first productive passages of P4 and P5, and the full-length genome of KNU-1807 at the later P10 passage. A unique 7-aa DEL in nsp3 identified in the original isolate was

TABLE 3 Comparison of the full-length genomes of 2018 Jeju isolates to the Korean G2b prototype KNU-1305 strain

Genome region (nucleotide length)	% Identity (no. of nt or aa differences) to KNU-1305						
	KNU-1804	KNU-1806	KNU-1807	KNU-1815	KNU-1816	KNU-1817	KNU-1818
5'-UTR (292)	98.6 (4)	99.6 (1)	98.9 (3)	98.2 (5)	98.2 (5)	99.6 (1)	98.2 (5)
ORF1ab (20,345)	99.5 (32)	99.4 (34)	99.3 (40)	99.4 (33)	99.3 (41)	99.5 (29)	99.4 (38)
nsp1 (363)	98.3 (2)	98.3 (2)	99.1 (1)	98.3 (2)	100 (0)	97.5 (3)	99.1 (1)
nsp2 (2,322)	99.6 (3)	99.7 (2)	99.2 (6)	99.4 (4)	98.8 (9)	99.7 (2)	99.4 (4)
nsp3 (4,863)	99.3 (11)	99.3 (10)	98.7 (14)	99.1 (11)	99.3 (11)	99.3 (10)	99.0 (16)
nsp4 (1,443)	99.5 (2)	99.3 (3)	99.1 (4)	99.1 (4)	98.3 (8)	99.5 (2)	99.1 (4)
nsp5 (906)	99.6 (1)	99.3 (2)	99.6 (1)	100 (0)	99.6 (1)	99.0 (3)	99.3 (2)
nsp6 (840)	99.6 (1)	99.2 (2)	98.5 (4)	99.2 (2)	98.2 (5)	99.6 (1)	98.5 (3)
nsp7 (249)	98.7 (1)	100 (0)	100 (0)	100 (0)	100 (0)	100 (0)	97.5 (2)
nsp8 (585)	99.4 (1)	99.4 (1)	100 (0)	100 (0)	100 (0)	99.4 (1)	100 (0)
nsp9 (324)	100 (0)	99.0 (1)	99.0 (1)	98.1 (2)	98.1 (2)	100 (0)	100 (0)
nsp10 (405)	100 (0)	100 (0)	100 (0)	100 (0)	100 (0)	100 (0)	99.2 (1)
nsp11 (54)	100 (0)	100 (0)	100 (0)	100 (0)	100 (0)	100 (0)	100 (0)
nsp12 (2,781)	99.8 (1)	99.7 (2)	99.6 (3)	99.8 (1)	100 (0)	99.7 (2)	99.8 (1)
nsp13 (1,791)	99.4 (3)	99.4 (3)	99.8 (1)	99.8 (1)	99.6 (2)	99.6 (2)	99.6 (2)
nsp14 (1,551)	99.6 (2)	99.6 (2)	99.4 (3)	99.6 (2)	100 (0)	100 (0)	100 (0)
nsp15 (1,017)	99.1 (3)	98.8 (4)	99.4 (2)	98.8 (4)	99.4 (2)	99.1 (3)	99.7 (1)
nsp16 (906)	99.6 (1)	100 (0)	100 (0)	100 (0)	99.6 (1)	100 (0)	99.6 (10)
Spike (4,161)	98.3 (23)	98.2 (24)	98.2 (24)	98.1 (25)	98.1 (22)	98.3 (23)	97.9 (28)
ORF3 (675)	99.5 (1)	98.6 (3)	98.2 (4)	98.6 (3)	98.2 (4)	99.1 (2)	99.5 (1)
E (231)	98.6 (1)	98.6 (1)	100 (0)	100 (0)	98.6 (1)	97.3 (2)	100 (0)
M (681)	99.5 (1)	100 (0)	99.1 (2)	100 (0)	98.2 (4)	98.6 (3)	100 (0)
N (1,326)	99.5 (2)	99.7 (1)	98.6 (6)	99.0 (4)	98.4 (7)	99.3 (3)	98.6 (6)
3'-UTR (334)	99.7 (1)	100 (0)	100 (0)	99.4 (2)	99.7 (1)	99.7 (1)	98.5 (5)
Total	99.4 (4/60/1) ^a	99.3 (1/63/0)	99.3 (3/76/0)	99.3 (5/65/2)	99.3 (5/79/1)	99.3 (1/62/1)	99.4 (5/73/5)

^aThe number of individual differences in the 5'-UTR, protein-coding region, and 3'-UTR, respectively.

stable upon serial passages in cell culture. The S sequence analysis of the P4 isolate of KNU-1807 (KNU-1807-P4) compared to the original KNU-1807-SI sample revealed that KNU-1807-P4 acquired 3-nt substitutions that resulted in two non-synonymous changes (Phe to Leu and Lys to Arg) at aa positions 501 and 614 respectively. Strikingly, a continuous 8-nt DEL was identified in the C-terminal region of the S gene of KNU-1807-P4 at genomic positions 24,742–24,749, leading to a frameshift that caused an alternative TGA termination codon upstream of the authentic termination of S (Figure 4a). As a result of the early termination, a 9-aa truncated cytoplasmic domain (S C-DEL9) and one aa mutation (Y1377F) at the last position of the S gene product were generated compared to that of KNU-1807-SI (Figure 4b and Table 4). These genetic alterations that occurred in P4 remained unchanged through P10 and no additional variations emerged in the S-coding region during the subsequent serial passages. The partial or complete genome sequences of all the cell culture-passaged viruses were compared to the original KNU-1807-SI and the results are summarized in Table 4.

3.3 | Pathogenicity of KNU-1807

Since the KNU-1807 strain with the truncated S cytoplasmic tail (KNU-1807-S C-DEL9) was isolated from a conventional pig farm that experienced moderate-scale neonatal mortality, we were interested in assessing its *in vivo* phenotypic characteristics. Thus, the pathogenicity of the KNU-1807-S C-DEL9 virus (KNU-1807-P10) compared to that of the virulent G2b strain was evaluated by experimental infection of newborn piglets. Nine piglets divided into three groups of three or four animals each were challenged orally with KNU-141112-P5 (group 1) or KNU-1807-P10 (group 2) and the remaining two piglets in a control group were inoculated with cell culture medium. Clinical signs were recorded three times daily and faecal swabs were collected prior to inoculation and daily after inoculation for the duration of the study. During the acclimation period, all piglets were active, showed no clinical symptoms and had normal faecal consistency, and their faecal samples were negative for PEDV RNA. Following viral challenge, none of the negative-control piglets

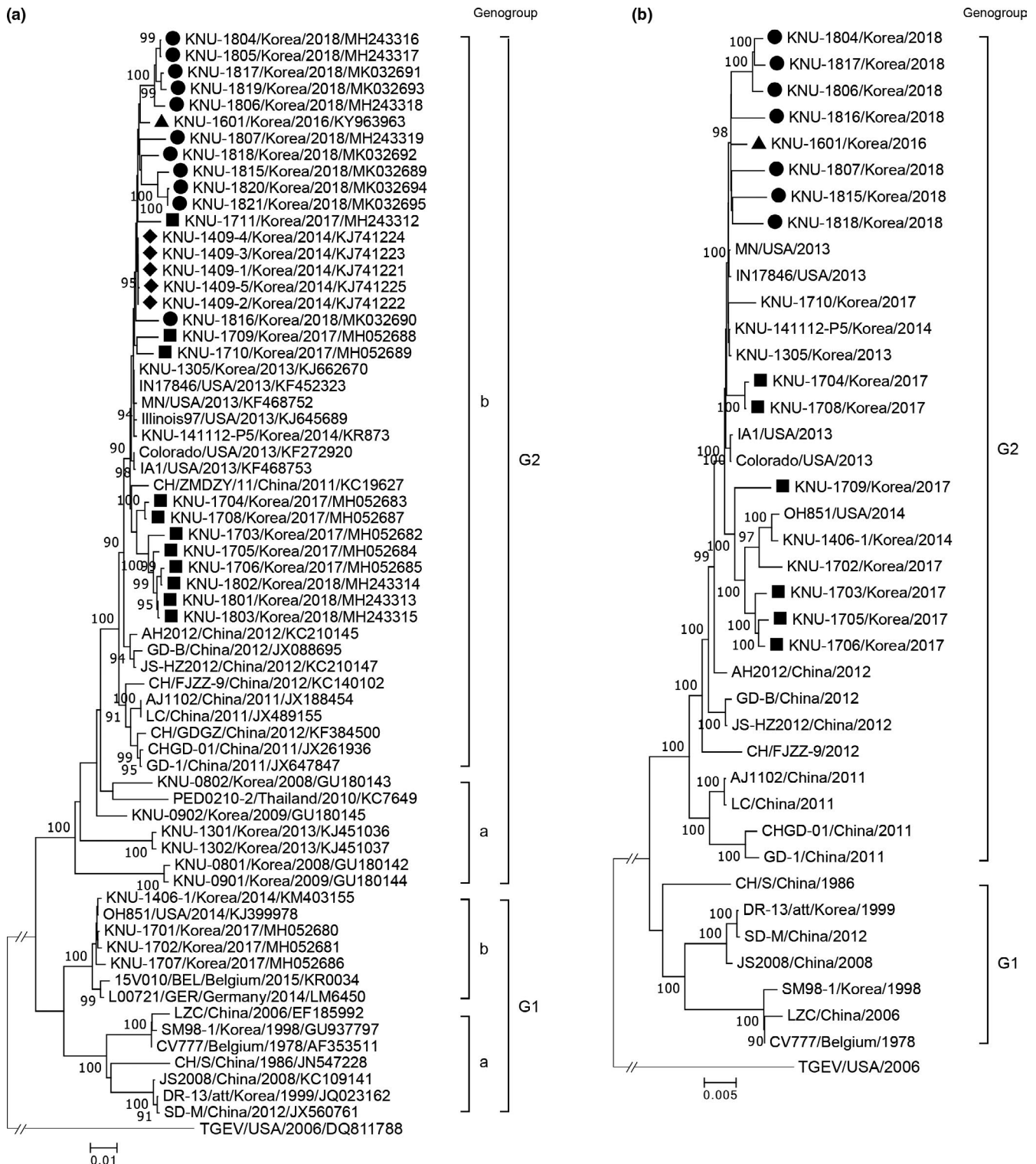


FIGURE 2 Phylogenetic analyses based on the nucleotide sequences of the spike (S) genes (a) and full-length genomes (b) of the PEDV strains. A region of the S gene and the complete genome sequence of TGEV were included as the outgroups in each tree. Multiple sequence alignments were performed using ClustalX software and phylogenetic trees were constructed from the aligned nucleotide sequences using the neighbour-joining method. Numbers at each branch are bootstrap values greater than 50% based on 1,000 replicates. The names of the strains, countries and dates (year) of isolation, GenBank accession numbers, and genogroups and subgroups proposed in this study are shown. Solid circles indicate the 2018 strains identified in this study; solid diamonds indicate the re-emergent Jeju strains identified in 2014; solid triangles indicate the recent strains identified on Jeju Island in 2016 and 2017; solid squares indicate the recent strains identified in mainland South Korea in 2017–2018. Scale bars indicate nucleotide substitutions per site

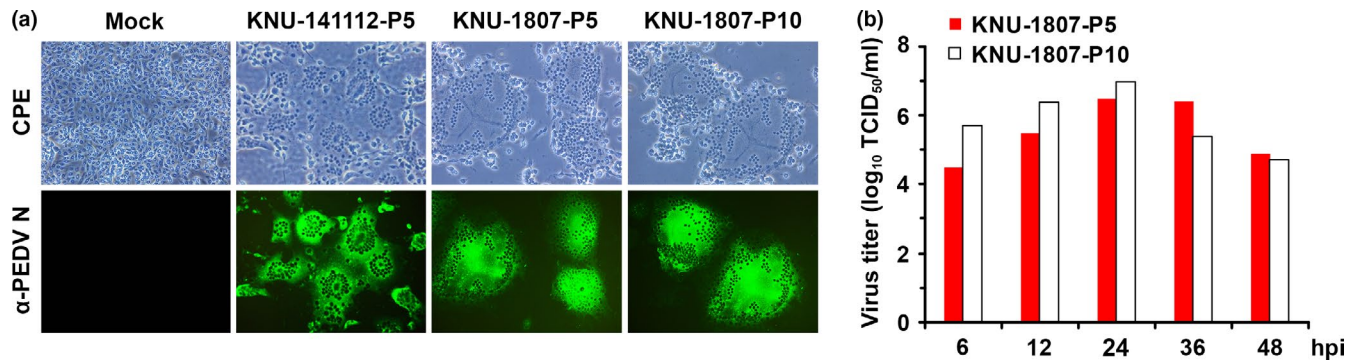


FIGURE 3 Cytopathology and growth properties of KNU-1807. (a) CPE formation in Vero cells infected with KNU-141112 or KNU-1807. PEDV-specific CPE were monitored daily and cells were photographed at 24 hpi using an inverted microscope at a magnification of 200 \times (top panels). For immunostaining, infected cells were fixed at 24 hpi and incubated with MAb against the N protein followed by incubation with Alexa green-conjugated goat anti-mouse secondary antibody (bottom panels). The cells were then nuclear stained with DAPI and examined using a fluorescence microscope at 200 \times magnification. (b) One-step growth kinetics for KNU-1807 strains. Vero cells were independently infected with PEDV KNU-1807-P5 and -P10. At the indicated time points post-infection, culture supernatants were harvested and virus titres were determined [Colour figure can be viewed at [wileyonlinelibrary.com](#)]



FIGURE 4 Nucleotide (a) and amino acid (b) sequence alignments of the C-terminal region of the S glycoprotein gene in PEDV classical G1a (purple colour) and virulent or cell-adapted attenuated G2b (block colour) strains. The N-terminal region of ORF3 is included in panel (a), and the stop codon (TGA or TAA) of S and the start codon of ORF3 are in bold. The dashes (-) indicate deleted sequences [Colour figure can be viewed at [wileyonlinelibrary.com](#)]

developed clinical signs. In contrast, all KNU-141112-P5-challenged piglets (group 1) exhibited clinical signs, including lethargy, anorexia, and diarrhoeic faeces by 24 hpi (mean CSS = 1.66) and experienced severe watery diarrhoea with vomiting thereafter (mean CSS > 3.0) (Figure 5a). PEDV-associated mortality occurred in two of the animals in group 1 at 88 hpi. Although the onset of clinical signs was 1-day delayed in the S C-DEL 9 virus-inoculated animals in group 2, they eventually developed PEDV-specific clinical symptoms from 32 or 40 hpi (mean CSS = 3). Only one animal in group 2 died from PEDV at 88 hpi, whereas the three remaining piglets experienced less severe watery diarrhoea from 96 dpi onward and remained alive until the termination of the study (Figure 5a). All the piglets in group 1 were tested positive for PEDV by RT-PCR at 1 dpi with

a mean Ct value of 25.3 (equivalent to $10^{2.23}$ TCID₅₀/ml) and they shed dramatically elevated levels of PEDV in their faeces starting at 2 dpi with Ct values ranging from 15.3–17.0 ($10^{5.8}$ – $10^{6.3}$ TCID₅₀/ml) (Figure 5b). In contrast, PEDV faecal shedding in all piglets in group 2 was recorded by 2 dpi with a mean Ct value of 18.5 ($10^{5.4}$ TCID₅₀/ml), which was maintained at similar levels through 5 dpi. Overall, a late onset and significant decline in quantities of faecal shedding for the first 2 days post-inoculation were observed in the animals of group 2 relative to those in the animals of group 1. Negative-control pigs remained healthy with normal faeces and no detectable PEDV shedding in faeces throughout the duration of the experiment.

All piglets in groups 1 and 2 that died at 4 dpi were necropsied, while the remaining animals that survived in the

TABLE 4 Nucleotide and amino acid changes of KNU-1807 during serial passages in cell culture

Genome region (nucleotide length)	Nucleotides				Amino acids			
	Position	SI	P4	P10	Position	SI	P4	P10
5' UTR (292)	– ^a	–	ND	–	–	–	ND	–
ORF1ab (20,324)	–	–	ND	–	–	–	ND	–
Spike (4,161)	1501	T	C	C	501	F	L	L
	1841	A	G	G	614	K	R	R
	3,111	G	A	A	1,037	–	–	–
	4,129 ^b	<u>TAC</u>	<u>TTT</u>	<u>TTT</u>	1,377	Y	F	F
ORF3 (675)	–	–	ND	–	–	–	ND	–
E (231)	–	–	ND	–	–	–	ND	–
M (681)	–	–	ND	–	–	–	ND	–
N (1,326)	–	–	ND	–	–	–	ND	–
3' UTR (334)	–	–	ND	–	–	–	ND	–

Note: ND, Not determined.

^aNo nucleotide or amino acid change found.

^b8-nt deletions at S gene positions 4,130–4,137.

KNU-1807-P10-infected and control groups were killed for post-mortem assessment at the end of the trial (Figure 6). All animals challenged with a virulent KNU-141112-P5 strain macroscopically displayed archetypal PED-like gross lesions. Their small intestines were distended with the accumulation of a yellowish watery content and presented with thin transparent intestinal walls as a result of villous atrophy (Figure 6a). Microscopic assessment showed that the small intestines from all piglets in group 1 were characterized by acute viral enteritis with a shortening and fusion of the small intestine villi and vacuolation of the superficial epithelial cells (Figure 6g). IHC staining detected PEDV antigen predominant in the cytoplasm of epithelial cells in atrophied villi in all segments of the small intestines (Figure 6m). Analogously, both dead and surviving animals infected with KNU-1807 in group 2 during the experimental period exhibited remarkable visible pathological intestinal lesions (Figure 6b–e), typical histopathological features of viral enteritis with villous atrophy (Figure 6h–k) and the presence of viral antigen (Figure 6n–q), comparable to those in group 1. Although the mean (\pm SDM) jejunal VH:CD ratios in both PEDV-inoculated groups were significantly lower than those in the uninoculated control group (>7), there were no significant differences in the jejunal VH:CD ratios between the inoculated groups: 1.3 ± 0.6 in group 1 (KNU-141112) and 2.1 ± 1.3 in group 2 (KNU-1807). Neither macroscopic or microscopic intestinal changes nor viral antigen were present in the negative-control piglets (Figure 6f, l, and r).

4 | DISCUSSION

In the current study, determined the complete genome sequences of PEDV isolates recovered from diarrhoeic piglets on Jeju Island where region-wide epidemics have recurred since the dreadful re-emergence of the virus in the region in 2014. Compared to the 2013–2014 Korean and Jeju re-emergent G2b strains, the 2018 Jeju

Island isolates contained 19–26-aa changes in the S glycoprotein, which were randomly and broadly distributed throughout the S1 and S2 domains. Interestingly, among those, a number of mutations in the 2018 Jeju Island strains were absent in the field strains responsible for the regional outbreaks in mainland South Korea during 2017–2018 (Figure 1a) (Lee & Lee, 2018). Furthermore, a large 7-aa or small 3-aa DEL was found within the nsp3 of several Jeju strains, which was similarly reported in the epidemic isolates identified in mainland South Korea in late 2017; however, these DELs were 6-aa or 10-aa shorter than the nsp3-DEL of the recent mainland strain KNU-1705 respectively (Figure 1b) (Lee & Lee, 2018). The phylogeny further revealed that the Jeju epidemic and endemic strains reported since 2014 comprised their own clade within the G2b subgroup. Thus, genetic and phylogenetic analyses indicated that the re-emergent G2b Jeju strains persistently underwent independent evolution on Jeju Island since 2014 (Figure S2) and has become endemic within the provincial pork industry.

Similar to other coronavirus replicase-encoded nsps, many PEDV nsps (nsp1, nsp3, nsp5, nsp7, nsp14, nsp15 and nsp16) function as interferon (IFN) antagonists that modulate the innate immune response (Wang et al., 2016; Zhang, Shi, & Yoo, 2016). Along with variations extensively dispersed throughout the S gene, it would be interesting to identify mutations in these nsp genes, including INDELs that possibly contribute to the pathogenesis of PEDV. A majority of the non-silent point mutations, which appeared to have resulted from their continuous accumulation in the field over the past 3–4 years, occurred in the ORF1ab region encoding 16 nsps, particularly in nsp3. These 29–41 variations seem to be significant since the cell culture-attenuated G2b strain contained only 4-aa changes over 100 serial passages when compared to the virulent parental strain (Lee et al., 2017). Although no INDELs arose in the attenuated G2b virus S DEL5/ORF3 (Lee et al., 2017), the attenuated G1a-derived vaccine strains possess an 8-aa DEL in nsp3, which overlaps or is located 12 or 18 aa downstream of those found in the recent G2b field

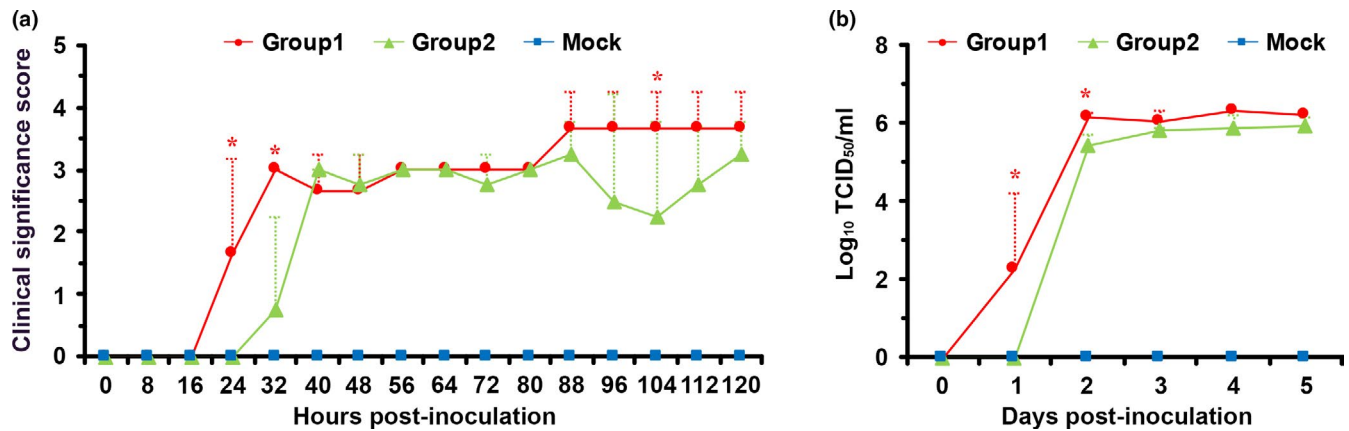


FIGURE 5 Clinical significance scores and virus shedding in piglets from three experimental groups. (a) Clinical significance scores were measured as described in the Materials and Methods section. (b) PEDV titres in rectal swap samples at each time point were determined by quantitative real-time RT-PCR analysis. The virus titres (\log_{10} TCID₅₀/ml) are the mean virus titres from all pigs and error bars represent the mean \pm *SDM*. *p* values were calculated by comparing the KNU-141112 virus- and KNU-1807 virus-inoculated groups using Student's *t* test. **p* < 0.05 [Colour figure can be viewed at wileyonlinelibrary.com]

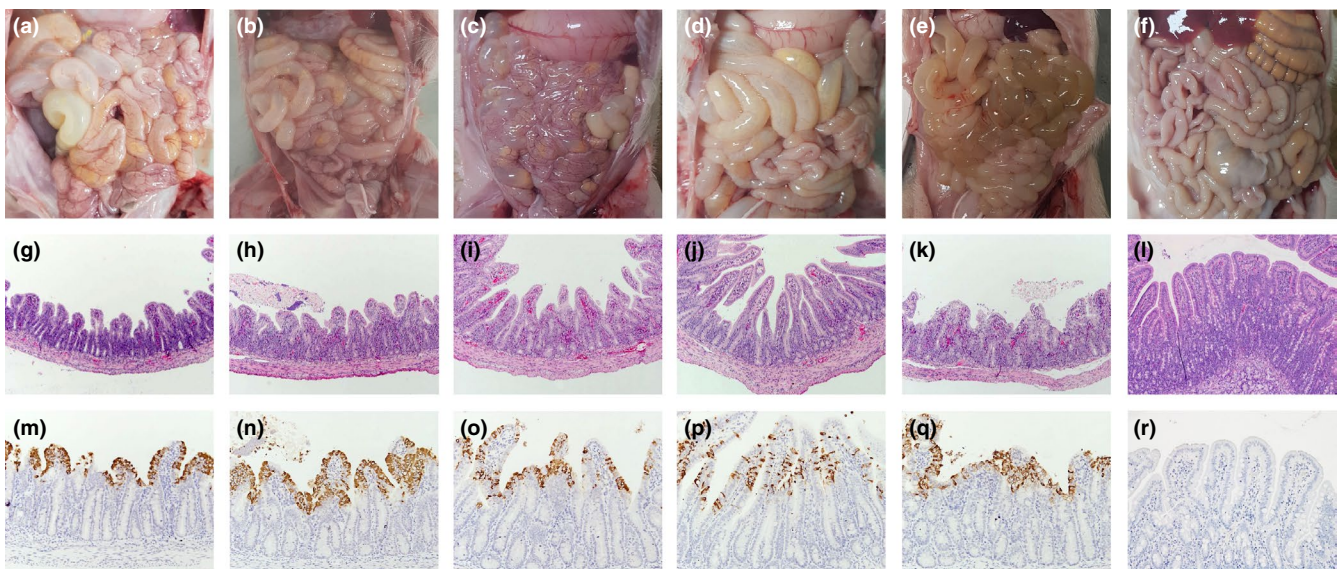


FIGURE 6 Macroscopic and microscopic small intestine lesions in piglets inoculated with the KNU-141112 and KNU-1807 strains. (a–f) Small intestines from representative pigs inoculated with KNU-141112-P5 (panel a) or KNU-1807 (panels b–e) and a negative-control animal (panel f) were examined for gross lesions. Note that piglets inoculated with the KNU-141112 or KNU-1807 virus typically presented with thin and transparent intestinal walls. (g–l) Haematoxylin and eosin-stained tissue sections of the jejunum from virus-inoculated and negative-control pigs (100 \times magnification). Jejunum specimens from piglets infected with the KNU-141112 or KNU-1807 strain showed acute diffuse atrophic enteritis with vacuolation of the superficial epithelial cells (panels g–k). The normal villous epithelium of the jejunum was recorded in the mock-inoculated piglet (panel l). (m–r) Detection of PEDV antigen by IHC analysis of the jejunum tissue sections from virus-inoculated and negative-control pigs (200 \times magnification). Immunostaining of PEDV antigen appears as brown staining and was detected in the epithelial cells of the jejunum in all PEDV KNU-141112- and KNU-1807-inoculated piglets (panels m–q). No PEDV antigen was detected in the jejunum of the mock-inoculated piglet (panel r) [Colour figure can be viewed at wileyonlinelibrary.com]

strains, implicating the potential involvement of the nsp3 DEL in attenuation (Figure 1b). Although nsp3 critically acts as a PL^{pro} that post-transcriptionally cleaves replicase polyproteins into functional nsps, the DELs present in the Glu-rich acidic region of nsp3 have no effect on its own roles and therefore are dispensable for the replication of coronaviruses, including PEDV (Lee & Lee, 2018; Lei, Kusov, & Hilgenfeld, 2018). Consistent with our previous study (Lee & Lee, 2018), this tolerance for the nsp3 DEL during PEDV replication was

reproduced in the current study as shown in Figure 3. Considering the genetic traits of nsp3, including homologous or heterologous DEL mutations, in addition with the heterogeneity of S genes, the nsp3 DEL pattern may be useful for investigating genetic relatedness and the molecular epidemiology of PEDV. In particular, the three isolates KNU-1815, -1820 and -1821, which were temporally and independently identified from three adjacent farms and shared 99.3%–100% identity with each other at the S gene level, were found

to contain a homologous 3-aa DEL in nsp3, consistent with a typical farm-to-farm transmission of PEDV via lax biosecurity.

In addition to genetic drift under field conditions, an outstanding DEL in the cytosolic endodomain of S was identified in the novel nsp3-DEL PEDV KNU-1807 isolate since the first productive passage in cell culture (P4) and subsequently retained, thereby resulting in a 9-aa DEL at the end of the KNU-1807-P4 S protein. Like other coronaviruses, the PEDV S glycoprotein can be functionally divided into two subdomains, S1 responsible for binding to cell receptor(s) and S2 involved in direct fusion between the viral and cellular membranes (Lee, 2015). The last 5-aa (KVHVQ) of the cytoplasmic tail of S is known to be a potential ER retrieval signal with its KxHxx motif and loss of this motif increases cell fusion activity by defecting the ER retention of S protein and promoting their transport to the cell surface (Lee et al., 2017; Lin et al., 2017; Shirato et al., 2011). Since KNU-1807-P4 exhibited a premature termination of the S protein by 9-aa residues (EVFEKVHVQ) that included the ER retrieval motif, it would be anticipated that this strain would demonstrate increased fusion activity *in vitro*. Our data revealed that the KNU-1807 strain produced significantly larger syncytia in infected cells compared to those observed in cells inoculated with PEDV containing an intact cytosolic domain of S (Figure 3a) (Lee et al., 2015). Similar DEL mutations at the end of S protein have been reported for the Korean G1a vaccine strain SM98-1 and cell culture-attenuated G2b strains KNU-141112-P80 (80-passage virus) and PC22A-P120 (120-passage virus) during *in vitro* serial passages (Lee et al., 2017; Lin et al., 2017). SM98-1 and KNU-141112-P80 have a large 52-nt or 46-nt DEL in the intergenic portion of S and ORF3, leading to the premature termination of S by 7-aa (FEKVHVQ) and 5-aa (KVHVQ) residues, respectively; whereas PC22A-P120 has a single nt substitution of GAA to TAA at positions 4,129–4,131 in the S gene, resulting in a stop codon and a 9-aa (EVFEKVHVQ) DEL. The S C-DEL9 identified in this study differed from aforementioned strains in that the early termination was caused by a combination of a novel nt DEL and a -1 frameshift event that occurred in the most primitive cell culture passage P4. It is possible that the S DEL naturally emerged during the initial culturing in the Vero cell via an unknown mechanism. Indeed, the occurrence of a large 197-aa S DEL in the N-terminus of the S protein that was absent in the original sample has been reported during the first cell culture passage of the US G2b PC177 strain (Oka et al., 2014). We were consistently unable to detect the same S C-DEL9 in the original KNU-1807-SI sample by deep genome sequencing (data not shown). However, since coronaviruses are known to innately exist as quasispecies or as mixed populations of several strains (Zhang et al., 2007), we cannot exclude the possibility that this variant was initially present as a minor proportion in the clinical sample and was able to replicate more competently in cell culture instead of the emergence of the extraordinarily DEL during the earliest stages of cell adaption. Similarly, a Chinese field G2b strain, FL2013, that naturally contains a unique 21-nt DEL in the extreme C-terminus of its S protein, leading to a 7-aa (FEKVHVQ)

S C-DEL pattern, has been found to have reduced virulence to newborn piglets (Zhang et al., 2015). Thus, it is important to further surveil whether S C-DEL variant strains naturally circulate in Korean pig populations.

Since a growing body of evidence proposes the early termination of the S protein and the extinction of its ER retention signal as being a marker for PEDV attenuation, we investigated whether the virulence of the KNU-1807 virus would be markedly less than that previously reported for PEDV pathogenesis. Our data revealed that despite similarities of macroscopic and microscopic small intestine lesions, the KNU-1807 virus possessed weakened pathogenicity in experimentally inoculated piglets compared to the virulent KNU-141112 strain in terms of disease severity of clinical presentation, including the mortality rate and onset of virus shedding, indicating the involvement of the extreme C-terminal region of the S protein in virulence. However, we were unable to observe a fully attenuated phenotypes for KNU-1807 in inoculated animals compared with those seen in our previous study (Lee et al., 2017). This suggested that DEL mutations in several parts of the S protein (N-terminal and C-terminal regions) and/or accessory ORF3 and/or nsp3 may affect the virulence of PEDV. Because comparative analysis of paired virulent/attenuated strains revealed no conserved patterns of attenuation-related genetic variations, it is less likely that point mutations throughout the genome significantly contribute to the change in virulence. Collectively, it is plausible that the complete attenuation of PEDV requires a combination of multiple genetic changes (mainly DELs) and that it consequently occurs as the result of simultaneous modification of multiple molecular and physiological mechanisms involved in pathogenesis. These aspects can be further assessed by using reverse genetics technology.

In conclusion, PEDV continues to endemically affect pig farms on Jeju Island, giving rise to moderate-to-severe clinical disease associated with PED in infected piglets. However, the loss of neonates to death varies among litters and between farms and is less than that reported for severe G2b epidemics, which approach 100% mortality in newborn piglets. This mild-to-moderate outbreak scenario seen on Jeju Island may be due to herd immunity developed from vaccination and intentional infection since the re-emergence of PEDV in the area. Another possibility is that genetic variation and/or DEL in nsps and S protein have arisen under field circumstances leading to the evasion of host immune defenses, such as IFN and neutralizing antibodies, and consequently alter viral pathogenicity, leading to endemic and low-pathogenic outbreaks in the field. Thus, cutting-edge research using reverse genetics will be necessary to provide fundamental insights into the specific role of nsp and S gene mutations in PEDV pathogenesis. More importantly, the current study confirmed that the contemporary field G2b isolates have nearly 4% amino acid sequence divergence in the S protein compared to the 2013–2014 domestic G2b strains. This mutation rate is approximately twice as high as that in recent mainland strains of PEDV (Lee & Lee, 2018). Furthermore, the evolutionary rate estimated for the S gene of PEDV G2b Jeju Island strains was 14.80×10^{-4} substitutions/site/year, whereas that for the G2b mainland strains was 7.18×10^{-4}

substitutions/site/year (Lee & Lee, 2018). These results indicated that ongoing genetic drift appears to be faster on Jeju Island than that on the South Korea mainland. This circumstance may alert the emergence of new genotypes or variant in the Jeju pig populations against which the current G2b vaccine may provide incomplete protection. This could lead to a 'counterattack' (reverse transmission) from Jeju Province to the mainland causing a recurrence of the 2013–2014 pandemics. Thus, novel variants may emerge via persistent genetic drifts during endemic outbreaks and may serve as a source for the resurgence of epizootics. This possibility remind us the necessity for monitoring and surveillance of the molecular epidemiology and aetiological characteristics of field PEDV isolates to identify and subsequently secure new vaccine seeds among them to predict and prepare for forthcoming national-wide or global epidemics. This study improves our understanding of the genetic diversity of PEDV field strains on Jeju Island and suggests that relatively swift and independent evolutionary processes continue to occur leading to the accumulation of non-lethal mutations indispensable for viral fitness in its host environment.

ACKNOWLEDGEMENT

This research was supported by the Basic Science Research Program through the National Research Foundation of Korea (NRF) funded by the Ministry of Education (NRF-2018R1D1A1B07040334).

CONFLICT OF INTEREST

The authors declare that they have no conflict of interest.

ORCID

Changhee Lee  <https://orcid.org/0000-0002-5930-5461>

REFERENCES

- Baek, P.-S., Choi, H.-W., Lee, S., Yoon, I.-J., Lee, Y. J., Lee, D. S., ... Lee, C. (2016). Efficacy of an inactivated genotype 2b porcine epidemic diarrhea virus vaccine in neonatal piglets. *Veterinary Immunology and Immunopathology*, *174*, 45–49. <https://doi.org/10.1016/j.vetimm.2016.04.009>
- Gorbalenya, A. E., Enjuanes, L., Ziebuhr, J., & Snijder, E. J. (2006). Nidovirales: Evolving the largest RNA virus genome. *Virus Research*, *117*, 17–37. <https://doi.org/10.1016/j.virusres.2006.01.017>
- Jung, K., Kim, J., Ha, Y., Choi, C., & Chae, C. (2006). The effects of transplacental porcine circovirus type 2 infection on porcine epidemic diarrhoea virus-induced enteritis in preweaning piglets. *Veterinary Journal*, *171*, 445–450. <https://doi.org/10.1016/j.tvjl.2005.02.016>
- Kim, S. H., Kim, I. J., Pyo, H. M., Tark, D. S., Song, J. Y., & Hyun, B. H. (2007). Multiplex real-time RT-PCR for the simultaneous detection and quantification of transmissible gastroenteritis virus and porcine epidemic diarrhea virus. *Journal of Virological Methods*, *146*, 172–177. <https://doi.org/10.1016/j.jviromet.2007.06.021>
- Lee, C. (2015). Porcine epidemic diarrhea virus: An emerging and re-emerging epizootic swine virus. *Virology Journal*, *12*, 193. <https://doi.org/10.1186/s12985-015-0421-2>
- Lee, C. (2019). Porcine epidemic diarrhoea virus. In H. Zakaryan (Ed.), *Porcine Viruses: From Pathogenesis to Strategies for Control* (pp. 107–134). Norfolk, UK: Caister Academic Press.
- Lee, D. K., Park, C. K., Kim, S. H., & Lee, C. (2010). Heterogeneity in spike protein genes of porcine epidemic diarrhea viruses isolated in Korea. *Virus Research*, *149*, 175–182. <https://doi.org/10.1016/j.virusres.2010.01.015>
- Lee, S., Kim, Y., & Lee, C. (2015). Isolation and characterization of a Korean porcine epidemic diarrhea virus strain KNU-141112. *Virus Research*, *208*, 215–224. <https://doi.org/10.1016/j.virusres.2015.07.010>
- Lee, S., Ko, D. H., Kwak, S. K., Lim, C. H., Moon, S. U., Lee, D. S., ... Lee, C. (2014). Reemergence of porcine epidemic diarrhea virus on Jeju Island. *Korean Journal of Veterinary Research*, *54*, 185–188. <https://doi.org/10.14405/kjvr.2014.54.3.185>
- Lee, S., & Lee, C. (2014). Outbreak-related porcine epidemic diarrhea virus strains similar to US strains, South Korea, 2013. *Emerging Infectious Diseases*, *20*, 1223–1226. <https://doi.org/10.3201/eid2007.140294>
- Lee, S., & Lee, C. (2017). Complete genome sequence of a novel S-insertion variant of porcine epidemic diarrhea virus from South Korea. *Archives of Virology*, *162*, 2919–2922. <https://doi.org/10.1007/s00705-017-3441-y>
- Lee, S., & Lee, C. (2018). Genomic and antigenic characterization of porcine epidemic diarrhoea virus strains isolated from South Korea, 2017. *Transboundary and Emerging Diseases*, *65*, 949–956. <https://doi.org/10.1111/tbed.12904>
- Lee, S., Son, K. Y., Noh, Y. H., Lee, S. C., Choi, H. W., Yoon, I. J., & Lee, C. (2017). Genetic characteristics, pathogenicity, and immunogenicity associated with cell adaptation of a virulent genotype 2b porcine epidemic diarrhea virus. *Veterinary Microbiology*, *207*, 248–258. <https://doi.org/10.1016/j.vetmic.2017.06.019>
- Lee, Y. N., & Lee, C. (2013). Complete genome sequence of a novel porcine parainfluenza virus 5 isolate in Korea. *Archives of Virology*, *158*, 1765–1772. <https://doi.org/10.1007/s00705-013-1770-z>
- Lei, J., Kusov, Y., & Hilgenfeld, R. (2018). Nsp3 of coronaviruses: Structures and functions of a large multi-domain protein. *Antiviral Research*, *149*, 58–74. <https://doi.org/10.1016/j.antiviral.2017.11.001>
- Lin, C.-M., Hou, Y., Marthaler, D. G., Gao, X., Liu, X., Zheng, L., ... Wang, Q. (2017). Attenuation of an original US porcine epidemic diarrhea virus strain PC22A via serial cell culture passage. *Veterinary Microbiology*, *201*, 62–71. <https://doi.org/10.1016/j.vetmic.2017.01.015>
- Oka, T., Saif, L. J., Marthaler, D., Esseili, M. A., Meulia, T., Lin, C.-M., ... Wang, Q. (2014). Cell culture isolation and sequence analysis of genetically diverse US porcine epidemic diarrhea virus strains including a novel strain with a large deletion in the spike gene. *Veterinary Microbiology*, *173*, 258–269. <https://doi.org/10.1016/j.vetmic.2014.08.012>
- Reed, L. J., & Muench, H. (1938). A simple method of estimating fifty percent endpoints. *American Journal of Epidemiology*, *27*, 493–497.
- Sagong, M., & Lee, C. (2011). Porcine reproductive and respiratory syndrome virus nucleocapsid protein modulates interferon- β production by inhibiting IRF3 activation in immortalized porcine alveolar macrophages. *Archives of Virology*, *156*, 2187–2195. <https://doi.org/10.1007/s00705-011-1116-7>
- Saif, L. J., Pensaert, M. B., Sestack, K., Yeo, S. G., & Jung, K. (2012). Coronaviruses. In B. E. Straw, J. J. Zimmerman, L. A. Krieger, A. Ramirez, K. J. Schwartz, & G. W. Stevenson (Eds.), *Diseases of Swine* (pp. 501–524). Ames, IA: Wiley-Blackwell.
- Saitou, N., & Nei, M. (1987). The neighbor-joining method: A new method for reconstructing phylogenetic trees. *Molecular Biology and Evolution*, *4*, 406–425.
- Shirato, K., Maejima, M., Matsuyama, S., Ujike, M., Miyazaki, A., Takeyama, N., ... Taguchi, F. (2011). Mutation in the cytoplasmic retrieval signal of porcine epidemic diarrhea virus spike (S) protein is responsible for enhanced fusion activity. *Virus Research*, *161*, 188–193. <https://doi.org/10.1016/j.virusres.2011.07.019>

- Stevenson, G. W., Hoang, H., Schwartz, K. J., Burrough, E. R., Sun, D., Madson, D., ... Yoon, K. J. (2013). Emergence of porcine epidemic diarrhea virus in the United States: Clinical signs, lesions, and viral genomic sequences. *Journal of Veterinary Diagnostic Investigation*, 25, 649–654. <https://doi.org/10.1177/1040638713501675>
- Tamura, K., Dudley, J., Nei, M., & Kumar, S. (2007). MEGA4: Molecular evolutionary genetics analysis (MEGA) software version 4.0. *Molecular Biology and Evolution*, 24, 1596–1599. <https://doi.org/10.1093/molbev/msm092>
- Thompson, J. D., Gibson, T. J., Plewniak, F., Jeanmougin, F., & Higgins, D. G. (1997). The ClustalX windows interface: Flexible strategies for multiple sequence alignment aided by quality analysis tools. *Nucleic Acids Research*, 25, 4876–4882. <https://doi.org/10.1093/nar/25.24.4876>
- Wang, D., Fang, L., Shi, Y., Zhang, H., Gao, L. I., Peng, G., ... Xiao, S. (2016). Porcine epidemic diarrhea virus 3C-like protease regulates its interferon antagonism by cleaving NEMO. *Journal of Virology*, 90, 2090–2101. <https://doi.org/10.1128/JVI.02514-15>
- Weng, L., Weersink, A., Poljak, Z., de Lange, K., & von Massow, M. (2016). An economic evaluation of intervention strategies for Porcine Epidemic Diarrhea (PED). *Preventive Veterinary Medicine*, 134, 58–68. <https://doi.org/10.1016/j.prevetmed.2016.09.018>
- Zhang, Q., Shi, K., & Yoo, D. (2016). Suppression of type I interferon production by porcine epidemic diarrhea virus and degradation of CREB-binding protein by nsp1. *Virology*, 489, 252–268. <https://doi.org/10.1016/j.virol.2015.12.010>
- Zhang, X., Hasoksuz, M., Spiro, D., Halpin, R., Wang, S., Vlasova, A., ... Saif, L. J. (2007). Quasispecies of bovine enteric and respiratory coronaviruses based on complete genome sequences and genetic changes after tissue culture adaptation. *Virology*, 363, 1–10. <https://doi.org/10.1016/j.virol.2007.03.018>
- Zhang, X., Pan, Y., Wang, D., Tian, X., Song, Y., & Cao, Y. (2015). Identification and pathogenicity of a variant porcine epidemic diarrhea virus field strain with reduced virulence. *Virology Journal*, 12, 88. <https://doi.org/10.1186/s12985-015-0314-4>

SUPPORTING INFORMATION

Additional supporting information may be found online in the Supporting Information section at the end of the article.

How to cite this article: Lee S, Lee D-U, Noh Y-H, et al. Molecular characteristics and pathogenic assessment of porcine epidemic diarrhoea virus isolates from the 2018 endemic outbreaks on Jeju Island, South Korea. *Transbound Emerg Dis*. 2019;66:1894–1909. <https://doi.org/10.1111/tbed.13219>